Using glutamine synthetase 1 to evaluate the symbionts' potential of ammonia assimilation and their responses to illumination in five organs of the giant clam, *Tridacna squamosa*

Leanne S. X. Teh[a, #], Jeslyn S. T. Poo [a, #], Mel V. Boo[a], Shit F. Chew[b] and Yuen K. Ip[a*]

[a]Department of Biological Sciences, National University of Singapore, Kent Ridge, Singapore 117543, Republic of Singapore

[b]Natural Sciences and Science Education, National Institute of Education, Nanyang Technological University, 1 Nanyang Walk, Singapore 637616, Republic of Singapore

[#]L.S. X. Teh and J.S. T. Poo have equal contributions to this study

[*]corresponding author

Running head: Dinoflagellate GS1 in *T. squamosa*

Correspondence address:
Dr. Y. K. Ip
Professor
Department of Biological Sciences
National University of Singapore
Kent Ridge
Singapore 117543
Republic of Singapore

Phone: (65)-6516-2702
Fax: (65)-6779-2486
Email: dbsipyk@nus.edu.sg

Abstract

Nitrogen-deficient symbiotic dinoflagellates (zooxanthellae) living inside the fluted giant clam, *Tridacna squamosa*, need to obtain nitrogen from the host. Glutamine synthetase 1 (GS1) is a cytosolic enzyme that assimilates ammonia into glutamine. We determined the transcript levels of *zooxanthellal GS1* (*Zoox-GS1*), which represented comprehensively *GS1* transcripts of *Symbiodinium*, *Cladocopium* and *Durusdinium*, in five organs of *T. squamosa*. The outer mantle had significantly higher transcript level of *Zoox-GS1* than the inner mantle, foot muscle, hepatopancreas and ctenidium, but the transcript ratios of *Zoox-GS1* to *zooxanthellal form II ribulose-1,5-bisphosphate carboxylase/oxygenase* (*Zoox-rbcII*), which represented the potential of ammonia assimilation relative to the phototrophic potential, were comparable among these five organs. Based on transcript ratios of *Zoox-GS1* to *zooxanthellal Urease* (*Zoox-URE*), the outer mantle had the highest potential of urea degradation relative to ammonia assimilation among the five organs, probably because urea degradation could furnish CO_2 and NH_3 for photosynthesis and amino acid synthesis, respectively, in the symbionts therein. The protein abundance of Zoox-GS1 was upregulated in the outer mantle and the inner mantle during illumination. Zoox-GS1 could catalyze light-enhanced glutamine formation using ammonia absorbed from the host or ammonia released through urea degradation in the cytoplasm. The glutamine produced could be used to synthesize other nitrogenous compounds, including amino acids in the cytoplasm or in the plastid of the dinoflagellates. Some of the amino acids synthesized by the symbionts in the inner mantle and foot muscle could be donated to the host to support shell organic matrix formation and muscle production, respectively.

Keywords: Glutamate, nitrogen, photosynthesis, protein, symbiotic dinoflagellates

List of abbreviations

DAPI 4′,6-diamidino-2-phenylindole

DIC differential interference contrast

GOGAT glutamine 2-oxoglutarate amidotransferase

GS1 glutamine synthetase 1

NDK nucleotide diphosphate kinase

SDS-PAGE sodium dodecyl sulfate polyacrylamide gel electrophoresis

PCA peptide competition assay

PPFD photosynthetic photon flux density

TPBS 0.05% Tween-20 in phosphate-buffered saline

***Zoox-rbcII*/Zoox-RBCII** zooxanthellal form II ribulose-1,5-bisphosphate carboxylase/oxygenase II

***Zoox-GS1*/Zoox-GS1** zooxanthellal glutamine synthetase 1

***Zoox-URE*/Zoox-URE** zooxanthellal Urease

1. Introduction

Dinoflagellates (Phylum: Myzozoa) are aquatic and unicellular alveolates (Kingdom: Alveloata) (Taylor et al., 2008). Most of them are free-living, but members of Family Symbiodiniaceae can live in symbiosis as zooxanthellae in animal hosts like scleractinian corals, symbiotic sea anemones and giant clams, which are members of the tropical coral reef ecosystems. Symbiodiniaceae dinoflagellates are phototrophic, and their life cycles comprise two stages: the free-living motile flagellate stage and the stationary coccoid stage (Meier et al., 2007). Although tropical waters are scarce in nutrients due to a lack of overturn (De Goeij et al., 2013), phototrophic host-dinoflagellate associations can thrive in shallow tropical waters where they can receive adequate irradiance.

Giant clams represent clam-dinoflagellate associations found in reef ecosystems of the Indo-Pacific. The majority of them harbor three genera of symbiotic dinoflagellates (DeBoer et al., 2012; Hernawan, 2008; Ikeda et al., 2017; Lim et al., 2019; Weber, 2009), *Symbiodinium*, *Cladocopium*, and *Durusdinium* (LaJeunesse et al., 2018), in various proportions. The establishment of a mutualistic association begins when the clam host ingests the motile symbiotic dinoflagellates, which then transform into coccoids without flagella. These symbionts reside extracellularly in a branched tubular system surrounded by hemolymph (Norton et al., 1992). The highest density of tertiary zooxanthellal tubules, and hence the majority of symbionts, are located in the colourful, extensible and fleshy outer mantle. The outer mantle is a distinctive feature of giant clams (Norton et al., 1992), as it uniquely contains iridocytes that can presumably scatter light of relevant wavelengths to the symbionts to promote photosynthesis (Holt et al., 2014) and protect the symbionts from harmful UV radiation (Rossbach et al., 2020). In the fluted giant clam, *Tridacna squamosa*, symbiotic dinoflagellates can also be found in organs located inside the mantle cavity, including the whitish inner mantle, foot muscle, ctenidium, and hepatopancreas (Poo et al., 2020, 2021). Particularly, relatively high densities of dinoflagellates are found in distinct regions near the hinge of the inner mantle

and at the tip of the foot muscle. Based on the transcript level of *zooxanthellal form II ribulose-1,5-bisphosphate carboxylase/oxygenase* (*Zoox-rbcII*), the outer mantle of *T. squamosa* has the greatest phototrophic potential. However, moderate levels of *Zoox-rbcII* are also expressed in the other four organs, although they lack iridocyte and have no direct exposure to light (Poo et al., 2020). During insolation, photosynthesizing dinoflagellates in the outer mantle can share a substantial portion of the photosynthates (~95%) with the host to satisfy its energy and metabolic needs (Fisher et al., 1985; Klumpp et al., 1992). As a result, the clam host can grow at relatively high rates and conduct light-enhanced shell formation (Ip et al., 2017; Rossbach et al., 2019), but it must supply essential nutrients (carbon, nitrogen and phosphorus) to the symbionts as they do not have access to the ambient seawater.

Nitrogen is needed by living organisms for the syntheses of amino acids, proteins, and nucleic acids. Free-living dinoflagellates can obtain nitrogen from the ambient seawater (Fuchinoue et al., 2012), and nitrogen is an indispensable component for chlorophyll biosynthesis in phototrophic dinoflagellates (Bernhard et al., 2010). By contrast, symbiotic dinoflagellates need to obtain nitrogen from the host. They have to synthesize amino acids not only for themselves, but also for the host that cannot produce essential amino acids (Wang and Douglas, 1999). As symbiotic dinoflagellates are nitrogen-deficient (Wilkerson and Trench, 1986), the clam host needs to absorb organic and inorganic nitrogen from the ambient seawater to benefit them. Indeed, the addition of inorganic nitrogen to the ambient seawater results in increased photosynthetic rate in symbionts and enhanced growth rate in the clam host (Hastie et al., 1992; Onate and Naguit, 1989; Summons et al., 1986).

Seawater contains dissolved inorganic nitrogen mainly as NH_4^+ and NO_3^-, as well as dissolved organic nitrogen in the form of urea and amino acids (Johannsson and Wedborg, 1980; Bronk et al., 2007). Some of these nitrogenous compounds are derived from the excretory nitrogenous wastes of aquatic animals (Campbell, 1991). Animals produce ammonia through the degradation of nitrogenous compounds, including amino acids, and ammonia must be

excreted or detoxified because of its toxicity (Campbell, 1991; Ip and Chew, 2010). Most aquatic animals excrete ammonia together with some urea (Campbell, 1991), but giant clams absorb ammonia and urea from seawater at rates faster in light than in darkness (Chan et al., 2018; Fitt et al., 1993a, b; Wilkerson and Trench, 1986). The absorption and assimilation of exogenous ammonia occur mainly in the host's ctenidium (Hiong et al., 2017a; Rees et al., 1994; Shepherd et al., 1999), which can assimilate the absorbed ammonia into glutamine through a host glutamine synthetase (GS; EC6.3.1.2). GS catalyzes the reaction NH_4^+ + glutamate + ATP → glutamine + ADP + P_i (Taylor and Curthoys, 2004). In the ctenidial epithelial cells of *T. squamosa*, the host GS has a cytosolic localization, and its transcript level and protein abundance increase significantly during 12 h of light exposure (Hiong et al., 2017a). Hence, exogenous ammonia absorbed by the ctenidium is supplied in the form of glutamine through the hemolymph to other host organs, including the outer mantle that contains a large population of symbionts inside zooxanthellal tubules.

Giant clams do not excrete ammonia under normal circumstances, except after exposure to extended periods of constant darkness (Muscatine and D'Elia, 1978; Szmant and Gassman, 1990; Wilkerson and Trench, 1986). Yet, they can maintain low ammonia concentrations in the hemolymph (Fitt et al., 1995), despite the production of ammonia through the degradation of nitrogenous compounds. This implies that the nitrogen-deficient symbiotic dinoflagellates must be able to salvage effectively the endogenous ammonia produced by the host, especially during illumination. Indeed, a novel cytosolic *GS1* sequence has been cloned from the symbiotic dinoflagellates residing in the outer mantle of *T. squamosa* (Fam et al., 2018). The deduced GS1 sequence is atypical as it contains an extra region characteristic of Nucleotide Diphosphate Kinase (NDK) and is therefore longer than other GSs. In addition, these dinoflagellates also express glutamine 2-oxoglutarate amidotransferase (GOGAT; or glutamate synthase; EC 1.4.1.13) in the plastid, which catalyzes the formation of two moles of glutamate from one mole of 2-oxoglutarate and one mole of glutamine (glutamine + 2-oxoglutarate + NADPH + H^+ →

148 2 glutamate + $NADP^+$) (Fam et al., 2018). With the glutamine synthetase 1:glutamate synthase
149 (GS1:GOGAT) cycle, symbiotic dinoflagellates can assimilate ammonia produced by the clam
150 host into glutamine and glutamate. They can also assimilate ammonia produced by themselves
151 through nitrate or urea metabolism. This can explain why intact giant clam-dinoflagellate
152 associations have low internal ammonia concentrations and do not excrete ammonia under
153 ordinary circumstances. As nitrogen plays an important role in the growth and physiology of
154 symbiotic dinoflagellates and their hosts (Belda et al., 1993; Belda and Yellowlees, 1995), it is
155 essential to estimate the potential of ammonia assimilation in symbionts residing in various
156 organs of *T. squamosa*. However, the possibility of the expression of *GS1*/GS1 in organs other
157 than the outer mantle of *T. squamosa* has not been explored, and the possibility of the gene and
158 protein expression levels of *GS1*/GS1 in these organs being regulated by illumination has not
159 been investigated.

160 Therefore, this study was performed to design a set of quantitative real-time PCR
161 (qPCR) primers that could react comprehensively with *GS1* from all three genera of symbiotic
162 dinoflagellates to determine the integral transcript levels of *zooxanthellal GS1* (*Zoox-GS1*),
163 which comprised *GS1* of of *Symbiodinium*, *Cladocopium* and *Durusdinium*, in the outer mantle,
164 inner mantle, foot muscle, hepatopancreas and ctenidium of *T. squamosa.* Based on results
165 obtained by Poo et al. (2021) on *rbcII*, the major species of *Symbiodinium, Cladocopium* and
166 *Durusdinium* present in these *T. squamosa* individuals obtained from Vietnam were
167 *Symbiodinium tridacnidorum* (ITS2 type A3), *Cladocopium* ITS2 type C92 and *Durusdinium*
168 *glynii* (ITS2 type D1), respectively. In addition, the transcript ratios of *Zoox-GS1*:*Zoox-rbclI*
169 (Poo et al., 2020) in these five organs were examined, in order to estimate the potential of
170 ammonia assimilation relative to the potential of carbon fixation. A similar analysis was
171 performed to obtain the transcript ratios of *Zoox-GS1:zooxanthellal Urease* (*Zoox-URE*; Ip et
172 al., 2020a) so as to compare the potential of ammonia assimilation relative to the potential of
173 urea assimilation in these five organs. The hypothesis tested was that symbiotic dinoflagellates

residing in these five organs of *T. squamosa* would have disparate potentials to assimilate ammonia with reference to the potentials of carbon fixation or urea assimilation. In addition, the transcript level and protein abundance of *Zoox-GS1*/Zoox-GS1 were determined in the outer mantle, inner mantle and foot muscle of individuals of *T. squamosa* kept in darkness for 12 h (control), or exposed to light for 3, 6 or 12 h. It was hypothesized that the expression levels of *Zoox-GS1*/Zoox-GS1 in some of these organs, particularly the outer mantle, could be up-regulated by illumination in order to facilitate the light-enhanced assimilation of ammonia into glutamine and other amino acids.

2. Materials and methods

2.1. Animals

Institutional (National University of Singapore Institutional Animal Care and Use Committee) approval was not required for research on giant clams. Adult *T. squamosa* weighing 550 ± 50 g (mean ± SD; n=28) were purchased from Xanh Tuoi Tropical Fish, Ltd (Vietnam). They were kept in three separate tanks (L90 cm x W62 cm x H60 cm), each containing 335 L of recirculating seawater. The water temperature and pH were ~26°C and 8.1-8.3, respectively. The other conditions are as follows: salinity, 30-32; hardness, 143–179 ppm; calcium, 380–420 ppm; total ammonia, <0.25 ppm; nitrate, 0 ppm; phosphate, <0.25 ppm. The shaded light intensity measured in water at the level of the giant clams was 120 PPFD (μmol m^{-2} s^{-1}), which is equivalent to the intensity adopted by Jantzen et al. (2008) to study *T. squamosa*. It would be ideal to expose giant clams individually to the experimental conditions, but in this study, individuals were sampled directly and randomly from the three glass tanks due to the limitation in the availability of re-circulating tanks and the need to keep them in the exact conditions, including salinity, water quality, and light intensity.

2.2. Exposure of animals to experimental conditions and tissue sample collection

To determine the transcript levels of *Zoox-GS1* in various organs of *T. squamosa*, ten clams were subjected to 3 h of light exposure before they were sacrificed for tissue sampling (n=10). A relatively large sample size (n=10) was used because the transcript levels of *Zoox-GS1* in some of the organs were low with substantial variation. Additionally, to investigate the effects of illumination on the expression of *Zoox-GS1*/Zoox-GS1, four clams were sampled at the end of a 12 h dark regime to serve as controls (n=4) while another twelve clams were subjected to either 3, 6, or 12 h of light exposure (n=4 for each condition) before tissue sampling. Giant clams were forced open for the cutting of the adductor muscle after they were anaesthetized with 0.2% phenoxyethanol. The outer mantle, inner mantle, foot muscle, hepatopancreas and

ctenidium were excised, blotted dry and freeze-clamped before storage at -80 °C until they were required for further processing. Tissue samples of the outer mantle of another two clams subjected to 12 h light were collected for immunofluorescence microscopy (n=2).

2.3. Antibody

An anti-Zoox-GS1 antibody that could react comprehensively with GS1 derived from *Symbiodinium*, *Cladocopium* and *Durusdinium* was custom-made by GenScript (Piscataway, NJ, USA). The epitope sequence (DGVTRSKTMTMTAR) was designed at a conserved region of five GS1 sequences obtained from four dinoflagellate databases (http://medinalab.org/zoox; http://marinegenomics.oist.jp/gallery/; http://marinegenomics.oist.jp/gallery/; http://palumbi.stanford.edu/data/). These five sequences included two *Symbiodinium* GS1 sequences from Bayer et al. (2012) and Shoguchi et al. (2018), two *Cladocopium* GS1 sequences obtained from Levin et al. (2016) and Shoguchi et al. (2018), and one *Durusdinium* GS1 sequence from Ladner et al. (2012). The selected epitope had 85.7-92.9% sequence similarity with these dinoflagellate GS1 sequences (Supplementary Table S1). Hence, it is probable that the anti-Zoox-GS1 antibody produced could react comprehensively with the GS1 sequences from *Symbiodinium*, *Cladocopium* and *Durusdinium*. In addition, an anti-α-tubulin antibody was also custom-made by GenScript based on the epitope of PKDVNAAVATIKTK. This epitope was selected based on alignment of various α-tubulin sequences obtained from multiple dinoflagellate databases (for the three genera of dinoflagellates) or Genbank (for various species of molluscs) (Supplementary Table S2). In theory, this anti-α-tubulin antibody would react with α-tubulin of the clam host and the dinoflagellates and could therefore act as a reference protein for Western blotting.

2.4. Immunofluorescence microscopy

Excised tissue samples of the outer mantle of *T. squamosa* were processed according to the protocol of Hiong et al. (2017b). Antigen retrieval was then conducted with 1% sodium dodecyl

sulfate in TPBS (0.05% Tween 20 in phosphate-buffered saline: 10 mmol l^{-1} Na_2HPO_4, 1.8 mmol l^{-1} KH_2PO_4, 137 mmol l^{-1} NaCl, 2.7 mmol l^{-1} KCl, pH 7.4) for 10 min. Thereafter, they were blocked with 1% bovine serum albumin in TPBS for 30 min at room temperature, followed with incubation overnight with custom-made anti-Zoox-GS1 rabbit polyclonal antibody at a dilution factor of 1:200 (5 μg ml^{-1} in TPBS). This was followed by incubation with the goat anti-rabbit Alexa Fluor 488 antibody at a dilution factor of 1:600 (3.33 μg ml^{-1} in TPBS) at 37°C for 1 h. Nucleus staining was then performed using 6-diamidino-2-phenylindole dihydrochloride (DAPI, Sigma-Aldrich Co., St Louis, MO, USA) for 10 min. The Olympus BX60 epifluorescence microscope equipped with an Olympus DP73 digital camera (Olympus Corporation, Tokyo, Japan) was used to capture microscopy images, which were subsequently processed with Adobe Photoshop CC (Adobe Systems, CA, USA). As dinoflagellates are known to display green auto-fluorescence of cellular structures such as the plastids and accumulation bodies under blue light excitation (using the Olympus U-WNIBA Blue Fluorescence Filter), such auto-fluorescence may potentially interfere with green immunolocalization of targeted proteins (Tang and Dobbs, 2007). Therefore, the concentration of the primary antibody and exposure time to capture green immunolabeling were carefully controlled in this study to avoid interference by green auto-fluorescence. A peptide competition assay (PCA) was performed to further validate that the observed green florescence was indeed the result of anti-Zoox-GS1 immunostaining.

2.5. RNA extraction and cDNA synthesis

TRI Reagent® (Sigma-Aldrich Co.) was used to extract total RNA from the outer mantle, inner mantle, foot muscle, hepatopancreas and ctenidium of *T. squamosa*. The RNA was purified using PureLink™ RNA Mini Kit (Invitrogen, Thermo Fisher Scientific Inc., Waltham, MA, USA). The concentration of the purified total RNA was measured using a Shimadzu BioSpec-nano spectrophotometer (Shimadzu Corporation, Tokyo, Japan). Electrophoresis was then

257 performed to confirm RNA integrity, after which the purified RNA was reverse-transcribed
258 into cDNA with the RevertAid^{TM} first-strand cDNA synthesis kit (Thermo Fisher Scientific
259 Inc.).

260 **2.6. Determination of transcript levels of *Zoox-GS1*, *Zoox-rbcII* and *Zoox-URE* by**
261 **quantitative real-time PCR (qPCR)**

262 There are two types of quantification methods for qPCR (Wong and Medrano, 2005). Absolute
263 quantification allows the expression of transcript in absolute numbers of copies, which requires
264 the construction of a standard curve based on calibrated amount of the template obtained
265 through cloning. In relative quantification, the expression of the gene of interest is normalized
266 to that of a housekeeping gene in the same sample (e.g., using the formula: $2^{\Delta\Delta CT}$; Livak and
267 Schmittgen, 2001). Comparison of the normalized data between the experimental and control
268 samples gives rise to a fold change (Wong and Medrano, 2005), which does not allow the
269 comparison of the quantity of *Zoox*-GS1 transcripts in different organs because the transcript
270 level of the reference gene could vary among various organs. However, one of our objectives
271 was to compare the level of *Zoox-GS1* transcript in various organs of *T. squamosa*. Hence, we
272 decided to adopt the method of absolute quantification of transcript level in this study.

273 A set of genera-comprehensive *Zoox-GS1* qPCR primers (forward: 5'-
274 GGAGCAAGGTCATGGAGGA-3'; reverse: 5'-GCCGCCGAACTTGATGAT-3') was
275 designed based on a conserved region of all *GS1* sequences available in various dinoflagellate
276 databases (http://medinalab.org/zoox; http://smic.reefgenomics.org/download;
277 http://marinegenomics.oist.jp/gallery/; http://palumbi.stanford.edu/data/). These include three
278 *Symbiodinium GS1* sequences (Aranda et al., 2016; Bayer et al., 2012; Shoguchi et al., 2018),
279 two *Cladocopium GS1* sequences (Levin et al., 2016; Shoguchi et al., 2018) and one
280 *Durusdinium GS1* sequence (Ladner et al., 2012). Therefore, this set of primers could probably
281 react comprehensively with all *GS1* sequences from *Symbiodinium*, *Cladocopium* and

Durusdinium (supplementary Table S3). The genera-comprehensive primers designed by Poo et al. (2020) for *Zoox-rbcII* (forward: 5'-CAGTTCTTGCACTACCACCG-3'; reverse: 5'-CATCTTGCCGAAGCTCATGG-3'), and the genera-comprehensive primers designed by Ip et al. (2020b) for *Zoox-URE* (forward: 5'-TGAACTTCGGCTTCTCTGG-3'; reverse: 5'-CCGTGTGGATGGTGATGG-3') were adopted in this study to quantify *Zoox-rbcII* and *Zoox-URE* transcripts, respectively.

Absolute quantification of transcripts was determined using a StepOnePlus™ Real-Time PCR System (Thermo Fisher Scientific Inc.) following the method of Hiong et al. (2017b). The qPCR reactions consisted of the following reagents: 5 µL of qPCRBIO SyGreen Mix Hi-ROX (PCR Biosystems Inc., Wayne, Pennsylvania, USA), 0.3 µmol L^{-1} of the designed forward and reverse primers, and various quantities of cDNA from the different organs or plasmid standards (for standard curve construction). The reagents make up a total volume of 10 µL. The cycling conditions consisted of an initial 20 s denaturation and enzyme activation at 95°C, 40 cycles of 95°C for 3 s and 60°C for 30 s. The amplification efficiencies of the primer sets for *Zoox-GS1*, *Zoox-rbcII* and *Zoox-URE* were 104.9%, 95.2% and 92.0% respectively. The quantification of *Zoox-GS1*, *Zoox-rbcII* or *Zoox-URE* transcripts in a sample was calculated from the corresponding linear regression line derived from three different standard curves and expressed as copy number per ng of total (dinoflagellate + host) RNA.

As the gene of interest in this study was *Zoox-GS1* derived from symbiotic dinoflagellates, the results of absolute quantification of transcript levels should traditionally be referenced specifically to the dinoflagellate RNA, and not the dinoflagellate + host RNA. However, the dinoflagellate RNA could be a variable factor among different organs of an individual giant clam or among the same organ (e.g. the outer mantle) of different individuals. Such variations could introduce problems to the comparison of results obtained from different organs or different individuals, if they were expressed as copy number per ng of total

dinoflagellate RNA. Moreover, the quantification of dinoflagellate RNA separated from the host RNA in tissues samples obtained from giant clams was not technically feasible. To resolve this problem, we decided to quantify the transcript levels of *Zoox-rbcII* and *Zoox-URE*, which were expressed solely by the symbiotic dinoflagellates and not the clam host. By calculating the transcript ratios of *Zoox-GS1*/*Zoox-rbcII* and *Zoox-GS1*/*Zoox-URE*, the denominators of total (dinoflagellate + host) RNA were cancelled, and the ratios obtained from different organs can be compared directly. Importantly, the ratios would provide information on the potential of ammonia assimilation with reference to the potential of photosynthesis or the potential of urea degradation in dinoflagellates residing in different organs of *T. squamosa*. However, *Zoox-rbcII* and *Zoox-URE* did not satisfy the criteria of a reference gene, as their transcript levels also varied in response to light exposure (Poo et al., 2020; Ip et al. 2020). Hence, it was inappropriate to express our results by the method of relative quantification in the format of $2^{\Delta\Delta CT}$ (Livak and Schmittgen, 2001).

2.7. SDS-PAGE and Western blotting

Extraction of proteins from the outer mantle, inner mantle and foot muscle of *T. squamosa* was performed following the steps mentioned in Hiong et al. (2017b). Proteins from the outer mantle (10 μg) and the inner mantle and foot muscle (100 μg each) were heated for 5 min at 95°C and run through 8% SDS-PAGE, before transfer onto nitrocellulose membranes. Western blotting was performed using the Pierce Fast Western Blot kit, SuperSignal® West Pico Substrate (Thermo Fisher Scientific Inc.). The anti-Zoox-GS1 antibody was diluted (1:2000) before incubating with the membrane at 25°C for 1 h. This was followed by incubation with optimized anti-rabbit horseradish peroxidase-conjugated secondary antibody at 25°C for 15 min. The chemiluminescence method was used to visualize bands using ChemiDoc™ Imaging Systems (Bio-Rad Laboratories, Hercules, CA, USA). The optical densities of bands of interest were analysed using ImageJ (version 1.50, NIH), and calibrated with a 37-step reflection

scanner scale (1” x 8” Stouffer #R3705-1C; Stouffer Graphic Arts, IN, USA). To validate the specificity of the anti-Zoox-GS1 antibody, peptide competition assay (PCA) was performed by incubating the immunizing peptide with anti-Zoox-GS1 antibody in a 5:1 ratio for 1 h prior to western blotting.

Based on traditional Western blotting methods, the optical density obtained for a targeted protein should theoretically be compared with the optical density of the band of a reference protein that would display constant abundance under control and experimental conditions. However, the situation is complex in this study, because the quantity of symbionts, and hence the abundance of the selected reference protein of dinoflagellate origin, would naturally vary between the same organs (the outer mantle) of different individuals of *T. squamosa*. As the outer mantle of *T. squamosa* comprised both host tissue and dinoflagellates, we had decided to use α-tubulin (host + dinoflagellates) as the reference protein. Hence, the protein abundance of Zoox-GS1 was expressed as the optical density of the Zoox-GS1 band normalized with reference to the optical density of the α-tubulin band.

2.8. Statistical analyses

All statistical tests were conducted with SPSS Statistics version 20 software (IBM Corporation, Armonk, NY, USA). The values presented as ratios were compared using the non-parametric Friedman test of differences followed by a Wilcoxon Signed-Rank Test. Differences among ratios were regarded as statistically significant when the p-value was less than 0.01 after Bonferroni adjustment. For other values presented as means + S.E.M., Levene’s test was used to test the homogeneity of variance, after which One-way Analysis of Variance (ANOVA) was carried out. Where equal variance could be assumed, Tukey’s test was conducted. Otherwise, Dunnett’s *T3* post-hoc test was used to examine differences among the means of the different experimental groups. Differences among means are regarded as statistically significant if the p-value is less than 0.05.

3. Results

3.1. Immunolabeling of Zoox-GS1 in the outer mantle of *T. squamosa*

The differential interference contrast (DIC) and autofluorescence (red channel) microscopy confirmed that symbiotic dinoflagellates are located inside zooxanthellal tubules in the outer mantle of *T. squamosa* (Fig. 1A). Zoox-GS1, which comprised GS1 of *Symbiodinium*, *Cladocopium* and *Durusdinium*, was immunolocalized (green immunofluorescence) in the cytoplasm of some symbiotic dinoflagellates in the outer mantle (Fig. 1B, C, D). In some cases, Zoox-GS1 immunofluorescence appeared to be associated with the plasma membrane of the symbionts (Fig. 1B, C, D), indicating that cytoplasmic Zoox-GS1 could be concentrated in regions near to the plasma membrane. The immunofluorescence of Zoox-GS1 immunolabelling could be abolished through a peptide competition assay (Fig. 1E).

3.2. Gene expression of Zoox-GS1 in five organs of *T. squamosa*

The transcript level of *Zoox-GS1*, which comprised *GS1* of *Symbiodinium*, *Cladocopium* and *Durusdinium*, in the outer mantle was the highest among the five organs studied (One-Way ANOVA, $F_{4,45}$=36.972, p-value=0.000; Fig. 2). Furthermore, the transcript level of *Zoox-GS1* in the inner mantle was significantly higher than those in the hepatopancreas and ctenidium, but comparable to that in the foot muscle (Fig. 2).

The transcript ratio of *Zoox-GS1* to *Zoox-rbcII* from the foot muscle was significantly higher than that from the hepatopancreas (Wilcoxon Signed-Rank Test, Z=-2.599, p-value=0.007; Table 1). On the other hand, the transcript ratios of *Zoox-GS1* to *Zoox-rbcII* from the inner mantle and the foot muscle were significantly higher than that from the outer mantle (inner mantle: Wilcoxon Signed-Rank Test, Z=-2.803, p-value=0.002, foot muscle: Wilcoxon Signed-Rank Test, Z=-2.701, p-value=0.004; Table 1).

3.3. Effects of light exposure on the transcript levels of Zoox-GS1 in five organs

The transcript ratio of *Zoox-GS1*, which comprised *GS1* of *Symbiodinium*, *Cladocopium* and *Durusdinium*, in the outer mantle of *T. squamosa* remained statistically unchanged after 3, 6 or 12 h of light exposure as compared with that of the control kept in the dark for 12 h (One-Way ANOVA, $F_{3,12}$=0.783, p-value=0.526; Fig 3A). By contrast, there was a significant increase in the transcript level of *Zoox-GS1* in the inner mantle at hour 3 of light exposure (One-Way ANOVA, $F_{3,12}$=13.476, p-value=0.000; Fig. 3B), but it returned to the control level after exposure to light for 12 h. On the other hand, the *Zoox-GS1* transcript level of the foot muscle decreased progressively and significantly between hour 3 and hour 6 of light exposure (One-Way ANOVA, $F_{3,12}$=29.544, p-value=0.000; Fig. 3C) and levelled off between hour 6 and hour 12. The transcript levels of *Zoox-GS1* in the hepatopancreas and ctenidium were too low for meaningful analyses of the effect of illumination.

3.4. Effects of light exposure on the protein abundance of Zoox-GS1 in five organs

Western blotting showed a band of interest at 85 kDa, which corresponded to the estimated molecular mass of Zoox-GS1 predicted from an online software (ExPASy SIB Bioinformatics Resource Portal). This band was eliminated after performing a peptide competition assay (Supplementary Fig. S1). The protein abundance of Zoox-GS1 was the highest in the outer mantle, followed by in the inner mantle and foot muscle. On the contrary, the 85 kDa band of interest was undetectable in extracts from the hepatopancreas and ctenidium at 100 μg of protein load (Supplementary Fig. S2).

When compared with the control kept in darkness for 12 h, there were significant increases in protein abundance of Zoox-GS1 in the outer mantle (One-Way ANOVA, $F_{3,12}$=17.212, p-value=0.000; Fig. 4A) and inner mantle (One-Way ANOVA, $F_{3,12}$=15.306, p-value=0.000; Fig. 4B) of *T. squamosa* after 12 h and 6 h of light exposure, respectively. By contrast, the protein abundance of Zoox-GS1 in the foot muscle remained statistically

405 unchanged throughout the 12-h period of light exposure (One-Way ANOVA, $F_{3,12}$= 0.865, p-
406 value=0.486; Fig. 4C).

4. Discussion

4.1. Symbiotic dinoflagellates need to share with the host essential and non-essential amino acids

It has been proposed that the cnidarian hosts of scleractinian corals can regulate the symbionts' population by controlling the availability of endogenous ammonia to them (Cui et al., 2019; Xiang et al., 2020), as it can recycle the metabolic ammonia into nonessential amino acids using the organic carbon-chains donated by the photosynthesizing symbionts (Cui et al., 2019; Falkowski et al., 1993). However, this proposition overlooks the fact that the cnidarian host also absorbs exogenous ammonia (Muscatine and D'Elia, 1978), urea (Grover et al., 2006) and NO_3^- (Franzisket, 1973) to benefit the photosynthesizing symbionts, and the rates of ammonia and urea absorption are higher in light than in darkness. Importantly, animals cannot synthesize all the twenty amino acids needed for growth development, and they must obtain nine essential amino acids (histidine, isoleucine, leucine, lysine, methionine, phenyalanine, threonine, tryptophan and valine) from the diet (Leuchtenberger et al., 2005). Although the symbiotic sea anemone, *Aiptasia pulchella*, can atypically synthesize methionine and threonine, it still needs to acquire seven essential amino acids from its symbionts (Wang and Douglas, 1999). Therefore, putting aside controlling the symbiont's population, the cnidarian host needs to provide the symbionts with an adequate supply of nitrogen in order to obtain the quantities of essential amino acids needed for growth and development from them. Otherwise, the host will need to depend on a combination of phototrophy and heterotrophy (i.e., mixotrophy) for survival.

Tridacna squamosa can live and grow in Millipore-filtered seawater for more than 10 months with light as the sole energy source (Fitt and Trench, 1981). This implies that the clam host can obtain all of the nutrients, including essential amino acids, from its phototrophic symbionts without resorting to mixotrophy (Klumpp and Griffiths, 1994). Particularly, the

clam host requires a large supply of amino acids for the production of muscle proteins, because muscles are needed for lateral movement (foot muscle), closing of the shell valves (adductor muscle), and retraction of the extended colourful outer mantle. It has been reported that the muscle of *T. squamosa* contains essential amino acids such as histidine, isoleucine, leucine, lysine, methionine, phenylalanine, threonine and valine (Liu et al., 2019). Hence, the clam host must supply the symbionts with the nitrogen needed for the synthesis of these amino acids. Indeed, *T. squamosa* conducts light-enhanced absorption of ammonia (Hiong et al., 2017a; Wilkerson and Trench, 1986), urea (Chan et al., 2018, 2019) and nitrate (Ip et al., 2020a) from the ambient seawater through its ctenidium. The absorbed urea and nitrate can be dedicated for the symbionts because the host cannot metabolize them. By contrast, the exogenous ammonia absorbed by the ctenidium is assimilated by the host's GS into glutamine (Hiong et al., 2017a) before making available to the symbionts. Hence, the ammonia circulating in the hemolymph or the intratubular fluid of the tubular system is probably produced endogenously by the host through the degradation of nitrogenous compounds. Our results indicate that symbiotic dinoflagellates residing in various organs of *T. squamosa* also express Zoox-GS1, and the protein abundance of Zoox-GS1 in the outer mantle and inner mantle could be upregulated by light exposure. Hence, the symbionts can increase the absorption and assimilation of endogenous ammonia produced by the host during illumination. This explains why giant clams do not excrete ammonia (Muscatine and D'Elia, 1978; Szmant and Gassman, 1990; Wilkerson and Trench, 1986) and why their hemolymph have only low concentrations of ammonia (Fitt et al., 1995).

4.2. Zoox-GS1 is localized in the cytoplasm and can be close to the plasma membrane of the symbiotic dinoflagellates in the outer mantle of *T. squamosa*

In plants, GS1 is located in the cytosol while GS2 is expressed in the chloroplast (Hirel and Gadal, 1981). Fam et al. (2018) reported that GS1 had a cytoplasmic localization in the

457 symbiotic dinoflagellates of *T. squamosa*, but their immunofluorescence images also indicated
458 a bit of green fluorescence, which could be autofluorescence, in some dinoflagellate organelles.
459 Green autofluorescence is known to be widespread among phototrophic and heterotrophic
460 dinoflagellates, diatoms, green algae, cyanobacteria, and raphidophytes (Carpenter et al., 1991;
461 Tang and Dobbs, 2007). It often occurs in eyespots, accumulation bodies, spines, and aerotopes
462 in the cytoplasm, and is caused by molecules unrelated to photosynthesis. Hence, efforts were
463 made in this study to avoid capturing autofluorescence during immunofluorescence
464 microscopy, and our results confirmed that Zoox-GS1 was indeed located in the cytoplasm of
465 dinoflagellates in the outer mantle of *T. squamosa*. Zoox-GS1 could be responsible for the
466 primary assimilation of absorbed ammonia to glutamine, or the re-assimilation of ammonia
467 produced through photorespiration or other reactions, in the cytoplasm of symbiotic
468 dinoflagellates. Our results have also showed that in some cases, GS was concentrated in
469 regions close to the plasma membrane. GS has been reported to be localized in the plasma
470 membrane (Kase et al., 2005). However, based on the GS1 sequence reported by Fam et al.
471 (2018), Zoox-GS1 does not consist of any transmembrane region or membrane anchor. Thus,
472 it is more likely that cytoplasmic Zoox-GS1 has some form of interaction with intrinsic proteins
473 embedded within the plasma membrane, similar to findings in soybean root nodules (Masalkar
474 et al., 2010). In such a location, Zoox-GS1 can turn the absorbed ammonia to glutamine to
475 maintain an inward-driven ammonia gradient for the continous uptake of ammonia.

476 **4.3. Multiple sources of nitrogen for symbiotic dinoflagellates—ammonia or urea?**

477 Our results, together with those of Ip et al. (2020b), indicate that symbiotic dinoflagellates in
478 different organs of *T. squamosa* could avoid competition for similar nitrogenous resources by
479 having disparate preferences to utilize a certain type of nitrogen-containing compound. By
480 virtue of its high density of symbiotic dinoflagellates and high exposure to irradiation, the outer
481 mantle had the highest transcript level of *Zoox-GS1* among the five organs studied. According

to Ip et al. (2020b), the outer mantle of *T. squamosa* also has the highest transcript level of *Zoox-URE* and ratio of *Zoox-URE*/*Zoox-rbcII*. Hence, symbiotic dinoflagellates residing in the outer mantle could have a greater potential to utilize urea with reference to their photosynthetic potential than those in other organs, and there could be a functional relationship between urea degradation and photosynthetic carbon-fixation (Ip et al., 2020b). By contrast, the ratio of *Zoox-GS1*/*Zoox-rbcII* in the outer mantle was comparable to those in the other four organs, denoting similar potential of ammonia assimilation in these five organs. Taken together, it becomes apparent that the potential of processing urea through URE is higher than that of processing ammonia through GS1 in the outer mantle of *T. squamosa*. Indeed, the ratio of *Zoox-GS1*/*Zoox-URE* in the outer mantle was significantly lower than those in other organs.

Why would it be advantageous for the symbionts of the outer mantle to have a higher potential to utilize urea-nitrogen than ammonia-nitrogen for amino acid synthesis? Zoox-URE is localized not only in the cytoplasm but also the plasma membrane and plastids of symbiotic dinoflagellates in *T. squamosa* (Ip et al., 2020b). The atypical localization of Zoox-URE in the plastid serves the important function of making available the urea-carbon, as CO_2, for photosynthesis (Ip et al., 2020b). Furthermore, this would allow symbiotic dinoflagellates to capture urea-nitrogen for the syntheses of amino acids inside the plastid, where carbon substrate, ATP, and reducing power can be provided conveniently by photosynthesis. As dinoflagellates of the inner mantle and foot muscle are known to have lower phototrophic potential than those in the outer mantle (Poo et al., 2020), the preference of metabolizing urea over ammonia would not provide these two organs with the advantage as in the case of the outer mantle.

4.4. Alignment of amino acid syntheses with photosynthesis in dinoflagellates of the outer mantle

In plants and algae, GS1 expression is regulated by light (Cantón et al., 1999; Tischner and Hüttermann, 1980). Similarly, the protein abundance of Zoox-GS1 in the outer mantle of *T. squamosa* was upregulated by light, even though the transcript level of *Zoox-GS1* remained unchanged. These results indicate that the expression of Zoox-GS1 was regulated at the translational level, and that illumination led to an increase in the potential of glutamine production in the outer mantle. Importantly, light-enhanced expression of Zoox-GS1 occurs in association with light-enhanced expression of Zoox-RBCII (Poo et al., 2020) and Zoox-URE (Ip et al., 2020b) in the outer mantle of *T. squamosa*. Hence, illumination augments the capacity of urea degradation (Zoox-URE), whereby the ammonia released could be assimilated into glutamine (Zoox-GS1) with the availability of carbon-chain during photosynthesis (Zoox-RBCII). In turn, glutamine produced in the cytoplasm can act as a key substrate for amino acid synthesis (Vander Heiden and DeBerardinis, 2017), or it can be translocated into the plastid to be processed by GOGAT for the production of glutamate (Fam et al., 2018). Glutamine and glutamate are essential substrates for the synthesis of many nitrogenous compounds essential for growth and development, including nucleic acids, cofactors, chlorophyll, glutathione and secondary metabolites (Moller, 2005; Newsholme et al., 2003). As the syntheses of these compounds require carbon-chains in addition to nitrogen, they need to occur concurrently with carbon fixation in photosynthesizing dinoflagellates of the outer mantle.

4.5. Dinoflagellates in the inner mantle produce glutamine needed by the host to synthesize organic matrix for shell formation

The whitish inner mantle of *T. squamosa* participates in light-enhanced shell-formation, as it is in direct contact with the extrapallial fluid where biomineralization occurs. Poo et al. (2020) have demonstrated the presence of a population of symbiotic dinoflagellates with low phototrophic potential at a special region of the inner mantle near to the hinge of the shell-valves of *T. squamosa*. Unlike those in the outer mantle, the gene and protein expression levels

of *Zoox-rbcII*/Zoox-RBCII in the inner mantle remain unchanged during light exposure (Poo et al., 2020). Why then, would the gene and protein expression levels of *Zoox-GS1*/Zoox-GS1 in the inner mantle of *T. squamosa* be upregulated by light?

Shell formation requires an organic matrix for the layered deposition of $CaCO_3$ onto the inner surface of the shell-valve (Greenfield et al., 1984). Protein is an important component of organic matrix and its synthesis requires amino acids. In the ass's-ear abalone, *Haliotis asinine*, the shell protein (or glycine-rich boundary protein) derived from the inner mantle is rich in glutamine (Marie et al., 2010). Amino acid analysis of the axial organic matrix obtained from corals reveals that proline and glutamine (24.0% and 28.9%) are the main building blocks of the matrix (Ehrlich et al., 2006). As the host must obtain glutamine and other amino acids needed for organic matrix synthesis from its symbionts, it would be advantageous for the inner mantle of *T. squamosa* to harbor a pool of symbionts that could upregulate the expression levels of *Zoox-GS1*/Zoox-GS1 to increase the potential of glutamine synthesis in support of light-enhanced shell formation. Unlike the outer mantle, the expression levels of *Zoox-GS1*/Zoox-GS1 in the inner mantle were regulated at both the transcriptional and translational level probably due to the relatively low transcript level of *Zoox-GS1* in control clams kept in darkness. The glutamine produced by this population of symbionts could be dedicated for shell formation, but these symbionts would need to obtain endogenous ammonia produced by the host, as well as glutamate and carbon-chains circulating in the luminal fluid of the tubular system.

4.6. Dinoflagellates in the foot muscle synthesize glutamine and other amino acids needed for protein synthesis in the host

The foot muscle of giant clam is instrumental to lateral movement (Huang et al., 2007; Stasek, 1962). Movement depends on muscle contraction, and muscle mass is contingent on the relative rates of protein synthesis and protein breakdown (Schiaffino et al., 2013). Therefore,

a balanced rate of protein synthesis must be sustained to maintain muscle mass, and a higher rate is required for muscle growth. Protein synthesis requires a supply of amino acids, and the clam host needs to obtain them from its symbiotic dinoflagellates. Indeed, the foot muscle of *T. squamosa* contains a concentrated population of symbiotic dinoflagellates at its tip, in spite of being shaded from light by the siphonal mantle, and has a low phototrophic potential (Poo et al., 2020). These symbionts could be specialized in producing amino acids to support protein synthesis in the foot muscle.

Notably, the foot muscle had slightly higher transcript level and protein abundance of *Zoox-GS1*/Zoox-GS1 than the inner mantle. It is uncertain why the transcript level of *Zoox-GS1* in the foot muscle would decrease during light exposure, but the unchanged protein abundance of Zoox-GS1 during 12 h of illumination shows that the potential of glutamine production remained constant in light or in darkness. This is unsurprising as the foot muscle is not known to display any light-dependent physiological phenomenon. Glutamine and glutamate are substrates for protein synthesis and they can also act as anabolic precursors for muscle growth (Newsholme et al., 2003). For instance, in blood clam, *Anadara broughtonii*, muscle tissue is characterized by higher percentage of glutamine than other soft tissues (Tabakaeva and Tabakaev, 2016). Hence, it is essential for symbionts in the foot muscle to absorb endogenous ammonia, glutamate and carbon-chains from the tubular fluid in order to synthesize glutamine through Zoox-GS1.

4.7. Perspective

Judging by the comprehensive transcript levels of *Zoox-GS1* derived from *Symbiodinium*, *Cladocopium* and *Durusdinium*, the capacity to assimilate ammonia relative to the phototrophic capacity (*Zoox-rbcII*) is comparable among the five organs studied. However, this does not necessarily imply that the contribution to the capacity of ammonia assimilation by the three individual genera of symbiotic dinoflagellates would be similar among these five organs. It is

important to examine whether there was a dominant genus of dinoflagellates from these *T. squamosa* specimens obtained from Vietnam, and to elucidate whether the potential to assimilate ammonia relative to the phototrophic potential would be different among *Symbiodinium*, *Cladocopium* or *Durusdinium* in the outer mantle and other organs. It is possible that these three genera of symbiotic dinoflagellates would have different expression levels of *GS1*/GS1 and hence different potential of assimilating ammonia into glutamine to benefit the host, the confirmation of which awaits future studies.

References

Aranda, M., Li, Y., Liew, Y.J., Baumgarten, S., Simakov, O., Wilson, M.C., Piel, J., Ashoor, H., Bougouffa, S., Bajic, V.B., Ryu, T., Ravasi, T., Bayer, T., Micklem, G., Kim, H., Bhak, J., LaJeunesse, T.C., Voolsra, C.R., 2016. Genomes of coral dinoflagellate symbionts highlight evolutionary adaptations conducive to a symbiotic lifestyle. Sci. Rep. 6, 39734.

Bayer, T., Aranda, M., Sunagawa, S., Yum, L.K., DeSalvo, M.K., Lindquist, E., Coffroth, M.A., Voolstra, C.R., Medina, M., 2012. *Symbiodinium* transcriptomes: genome insights into the dinoflagellate symbionts of reef-building corals. PLoS ONE 7(4), e35269.

Belda, C.A., Lucas, J.S., Yellowlees, D., 1993. Nutrient limitation in the giant clam-zooxanthellae symbiosis: effects of nutrient supplements on growth of the symbiotic partners. Mar. Biol. 117, 655–664.

Belda, C.A., Yellowlees, D., 1995. Phosphate acquisition in the giant clam-zooxanthellae symbiosis. Mar. Biol. 124, 261-266.

Bernhard, A., 2010. The nitrogen cycle: processes, players, and human impact. Nature Education Knowledge 2, 12.

Bronk, D.A., See, J.H., Bradley, P., Killberg, L., 2007. DON as a source of bioavailable nitrogen for phytoplankton. Biogeosciences 4, 283-296.

Campbell, J.W., 1991. Excretory nitrogen metabolism. Prosser, C. L. [Ed.] Environmental and Metabolic Animal Physiology, 4th edn. Comparative Animal Physiology. Wiley, New York, pp. 277-324.

Cantón, F.R., Suárez, M., Josè-Estanyol, M., Cánovas, F.M., 1999. Expression analysis of a cytosolic glutamine synthetase gene in cotyledons of Scots pine seedlings: developmental, light regulation and spatial distribution of specific transcripts. Plant Mol. Biol. 40, 623-634.

613 Carpenter, E.J., Chang, J., Shapiro, L.P., 1991. Green and blue fluorescing dinoflagellates in
614 Bahamian waters. Mar. Biol. 108, 145-149.
615 Chan, C.Y., Hiong, K.C., Boo, M.V., Choo, C.Y., Wong, W.P., Chew, S.F., Ip, Y.K., 2018.
616 Light exposure enhances urea absorption in the fluted giant clam, *Tridacna squamosa*,
617 and up-regulates the protein abundance of a light-dependent urea active transporter,
618 DUR3-like, in its ctenidium. J. Exp. Biol. 221(8), jeb176313.
619 Chan, C.Y., Hiong, K.C., Choo, C.Y., Boo, M.V., Wong, W.P., Chew, S.F., Ip, Y.K., 2019.
620 With illumination, the fluted giant clam, *Tridacna squamosa*, upregulates the protein
621 abundance of an apical Na^+: glucose cotransporter 1 homolog in its ctenidium, and
622 increases exogenous glucose absorption that can be impeded by urea. J. Exp. Biol. 222,
623 jeb195644.
624 Cui, G., Liew, Y,J., Li, Y., Kharbatia, N., Zahran, N.I., Emwas, A-H., et al., 2019. Host-
625 dependent nitrogen recycling as a mechanism of symbiont control in *Aiptasia*. PLoS
626 Genet. 15:e1008189. doi: 10.1371/journal.pgen.1008189
627 DeBoer, T.S., Baker, A.C., Erdmann, M.V., Jones, P.R., Barber, P.H., 2012. Patterns of
628 *Symbiodinium* distribution in three giant clam species across the biodiverse Bird's Head
629 region of Indonesia. Mar. Ecol. Prog. Ser. 444, 117-132.
630 De Goeij, J.M., Van Oevelen, D., Vermeij, M.J.A., Osinga, R., Middelburg, J.J., de Goeij,
631 A.F.P.M., Admiraal, W., 2013. Surviving in a marine desert: the sponge loop retains
632 resources within coral reefs. Science 342, 108–110.
633 Ehrlich, H., Etnoyer, P., Litvinov, S.D., Olennikova, M.M., Domaschke, H., Hanke, T., Born,
634 R., Meissner, H., Worch, H., 2006. Biomaterial structure in deep-sea bamboo coral
635 (Anthozoa: Gorgonacea: Isididae): perspectives for the development of bone implants
636 and templates for tissue engineering. Materialwissenschaft und Werkstofftechnik 37,
637 552-557.

638 Falkowski, P.G., Dubinsky, Z., Muscatine, L., McCloskey, L., 1993. Population control in
639 symbiotic corals. BioScience 43, 606-611.
640 Fam, R.R., Hiong, K.C., Choo, C.Y., Wong, W.P., Chew, S.F., Ip, Y.K., 2018. Molecular
641 characterization of a novel algal glutamine synthetase (GS) and an algal glutamate
642 synthase (GOGAT) from the colorful outer mantle of the giant clam, *Tridacna squamosa*,
643 and the putative GS-GOGAT cycle in its symbiotic zooxanthellae. Gene 656, 40-52.
644 Fisher, C.R., Fitt, W.K., Trench, R.K., 1985. Photosynthesis and respiration in *Tridacna gigas*
645 as a function of irradiance and size. Biol. Bull. 169, 230-245.
646 Fitt, W.K., Trench, R.K., 1981. Spawning, development, and acquisition of zooxanthellae by
647 *Tridacna squamosa* (Mollusca, Bivalvia). Biol. Bull. 161, 213-235.
648 Fitt, W.K., Heslinga, G.A., Watson, T.C., 1993a. Utilization of dissolved inorganic nutrients
649 in growth and mariculture of the tridacnid clam *Tridacna derasa*. Aquaculture 109, 27-
650 38.
651 Fitt, W.K., Rees, T.A.V., Braley, R.D., Lucas, J.S., Yellowlees, D., 1993b. Nitrogen flux in
652 giant clams: size-dependency and relationship to zooxanthellae density and clam biomass
653 in the uptake of dissolved inorganic nitrogen. Mar. Biol. 117, 381-386.
654 Fitt, W.K., Rees, T.A.V., Yellowlees, D., 1995. Relationship between pH and the availability
655 of dissolved inorganic nitrogen in the zooxanthella-giant clam symbiosis. Limnol.
656 Oceanogr. 40, 976-982.
657 Franzisket, L., 1973. Uptake and accumulation of nitrate and nitrite by reef corals.
658 Naturwissenschaften 60, 552.
659 Fuchinoue, Y., Katayama, T., Obata, M., Murata, A., Kinzie III, R., Taguchi, S., 2012. Growth,
660 biochemical properties, and chlorophyll fluorescence of symbiotic and free-living
661 dinoflagellates in response to ammonium enrichment. J. Exp. Mar. Biol. Ecol. 438, 01-
662 06.

663 Furla, P., Allemand, D., Shick, J.M., Ferrier-Pagès, C., Richier, S., Plantivaux, A., Merle, P.,
664 Tambutté, S., 2005. The symbiotic anthozoan: a physiological chimera between alga and
665 animal. Integ. Comp. Biol. 45, 595-604.
666 Greenfield, E.M., Wilson, D.C., Crenshaw, M.A., 1984. Ionotropic nucleation of calcium
667 carbonate by molluscan matrix. Am. Zool. 24, 925-932.
668 Grover, R., Maguer, J-F., Allemand, D., Ferrier-Pagès, C., 2006. Urea uptake by the
669 scleractinian coral *Stylophora pistillata*. J. Exp. Mar. Bio. Ecol. 332, 216-225.
670 Hastie, L.C., Watson, T.C., Isamu, T., Heslinga, G.A., 1992. Effect of nutrient enrichment on
671 *Tridacna derasa* seed: dissolved inorganic nitrogen increases growth rate. Aquaculture
672 106, 41-49.
673 Hernawan, U.E., 2008. Symbiosis between the giant clams (Bivalvia: Cardiidae) and
674 zooxanthellae (Dinophyceae). Biodiversitas 9, 53-58.
675 Hiong, K.C., Choo, C.Y.L., Boo, M.V., Ching, B., Wong, W.P., Chew, S.F., Ip, Y.K., 2017a.
676 A light-dependent ammonia-assimilating mechanism in the ctenidia of a giant clam.
677 Coral Reefs 36, 311-323.
678 Hiong, K.C., Cao-Pham, A.H., Choo, C.Y.L., Boo, M.V., Wong, W.P., Chew, S.F., Ip, Y.K.,
679 2017b. Light dependent expression of a Na^+/H^+ exchanger 3-like transporter in the
680 ctenidium of the giant clam, *Tridacna squamosa*, can be related to increased H^+ excretion
681 during light-enhanced calcification. Physiol. Rep. 5, e13209.
682 Hirel, B., Gadal, P., 1981. Glutamine synthetase isoforms in pea leaves: intracellular
683 localization. Zeitschrift für Pflanzenphysiologie 102, 315-319.
684 Holt, A.L., Vahidinia, S., Gagnon, Y.L., Morse, D.E., Sweeney, A.M., 2014. Photosymbiotic
685 giant clams are transformers of solar flux. J. R. Soc. Interface 11, 20140678.
686 Huang, D., Todd, P.A., Guest, J.R., 2007. Movement and aggregation in the fluted giant clam
687 (*Tridacna squamosa* L.). J. Exp. Mar. Biol. Ecol. 342, 269-281.

688 Ikeda, S., Yamashita, H., Kondo, S.N., Inoue, K., Morishima, S.Y., Koike, K., 2017.
689 Zooxanthellal genetic varieties in giant clams are partially determined by species-
690 intrinsic and growth-related characteristics. PloS One 12, e0172285.
691 Ip, Y.K., Chew, S.F., 2010. Ammonia production, excretion, toxicity, and defence in fish: a
692 review. Front. Physiol. 1, 134.
693 Ip, Y.K., Ching, B., Hiong, K.C., Choo, C.Y.L., Boo, M.V., Wong, W.P., Chew, S.F., 2015.
694 Light induces changes in activities of Na^+/K^+-ATPase H^+/K^+-ATPase and glutamine
695 synthetase in tissues involved directly or indirectly in light-enhanced calcification in the
696 giant clam *Tridacna squamosa.* Front Physiol. 6, 68.
697 Ip, Y.K., Hiong, K.C., Goh, E.J., Boo, M.V., Choo, C.Y., Ching, B., Wong, W.P., Chew, S.F.,
698 2017. The whitish inner mantle of the giant clam, *Tridacna squamosa*, expresses an
699 apical Plasma Membrane Ca^{2+}-ATPase (PMCA) which displays light-dependent gene
700 and protein expressions. Front. Physiol. 8, 781.
701 Ip, Y.K., Hiong, K.C., Teng, J.H., Boo, M.V., Choo, C.Y., Wong, W.P., Chew, S.F., 2020a.
702 The fluted giant clam (*Tridacna squamosa*) increases nitrate absorption and upregulates
703 the expression of a homolog of SIALIN (H^+: $2NO_3^-$ cotransporter) in the ctenidium
704 during light exposure. Coral Reefs 39, 451-465.
705 Ip, Y.K., Teng, G.C.Y., Boo, M.V., Poo, J.S.T., Hiong, K.C., Kim, H., Wong, W.P., Chew,
706 S.F., 2020b. Symbiodiniaceae dinoflagellates express urease in three subcellular
707 compartments and upregulate its expression levels in situ in three organs of a giant clam
708 (*Tridacna squamosa*) during illumination. J. Phycol. 56, 1696–1711.
709 DOI:10.1111/jpy.13053
710 Jantzen, C., Wild, C., El-Zibdah, M., Roa-Quiaoit, H.A., Haacke, C., Richter, C., 2008.
711 Photosynthetic performance of giant clams, *Tridacna maxima* and *T. squamosa*, Red Sea.
712 Mar. Biol. 155, 211-221.

713 Johansson, O., Wedborg, M., 1980. The ammonia-ammonium equilibrium in seawater at
714 temperatures between 5 and 25 C. J. Solution Chem. 9, 37-44.
715 Kase, S., Saito W., Yokoi, M., Yoshida, K., Furudate, N., Muramatsu, M., Saito, A., Kase, M.,
716 Ohno. S., 2006. Expression of glutamine synthetase and cell proliferation in human
717 idiopathic epiretinal membrane. Br. J. Ophthalmol. 90, 96-98.
718 Klumpp, D.W., Bayne, B.L., Hawkins, A.J. S., 1992. Nutrition of the giant clam *Tridacna*
719 *gigas* (L.) I. Contribution of filter feeding and photosynthates to respiration and growth.
720 J. Exp. Mar. Biol. Ecol. 155, 105-122.
721 Klumpp, D.W., Griffiths, C.L., 1994. Contributions of phototrophic and heterotrophic nutrition
722 to the metabolic and growth requirements of four species of giant clam (Tridacnidae).
723 Mar. Ecol. Progr. Ser. 115, 103-115.
724 Ladner, J.T., Barshis, D.J., Palumbi, S.R., 2012. Protein evolution in two co-occurring types
725 of *Symbiodinium*: an exploration into the genetic basis of thermal tolerance in
726 *Symbiodinium* clade D. BMC Evol. Bio. 12, 217.
727 LaJeunesse, T.C., Parkinson, J.E., Gabrielson, P.W., Jeong, H.J., Reimer, J.D., Voolstra, C.R.,
728 Santos, S.R., 2018. Systematic revision of Symbiodiniaceae highlights the antiquity and
729 diversity of coral endosymbionts. Curr. Biol. 28, 2570-2580.
730 Leuchtenberger, W., Huthmacher, K., Drauz, K., 2005. Biotechnological production of amino
731 acids and derivatives: Current status and prospects. Appl. Microbiol. Biot. 69, 01-08.
732 Levin, R.A., Beltran, V.H., Hill, R., Kjelleberg, S., Mcdougald, D., Steinberg, P.D., van Oppen,
733 M.J.H., 2016. Sex, scavengers, and chaperones: transcriptome secrets of divergent
734 *Symbiodinium* thermal tolerances. Mol. Biol. Evol. 33, 2201–2215.
735 Lim, S.S.Q., Huang, D., Soong, K., Neo, M.L., 2019. Diversity of endosymbiotic
736 Symbiodiniaceae in giant clams at Dongsha Atoll, northern South China Sea. Symbiosis
737 78, 251-262.

738 Liu, C., Li, T., Liu, E., Li, C., Wang, A., Gu, Z., 2019. Proximate Composition, Amino Acid
739 Content, and Fatty Acid Profile of the Adductor Muscle and Mantle from Two Species
740 of the Giant Clams Tridacna crocea and Tridacna squamosa. J. Shellfish Res. 38, 529-
741 534.
742 Livak, K.J., Schmittgen, T.D., 2001. Analysis of relative gene expression data using real-time
743 quantitative PCR and the $2^{-2\Delta\Delta Ct}$ method. Methods 25, 402-408.
744 Marie, B., Marie, A., Jackson, D.J., Dubost, L., Degnan, B.M., Milet, C., Marin, F., 2010.
745 Proteomic analysis of the organic matrix of the abalone *Haliotis asinina* calcified shell.
746 Proteome Sci. 8, 54.
747 Masalkar, P., Wallace, I. S., Hwang, J. H., Roberts, D. M., 2010. Interaction of cytosolic
748 glutamine synthetase of soybean root nodules with the C-terminal domain of the
749 symbiosome membrane nodulin 26 aquaglyceroporin. J. Biol. Chem. 285, 23880-23888.
750 Meier, K.J.S., Young, J.R., Kirsch, M., Feist-Burkhardt, S., 2007. Evolution of different life-
751 cycle strategies in oceanic calcareous dinoflagellates. Eur. J. Phycol. 42, 81-89.
752 Miller, D.J., Yellowlees, D., 1989. Inorganic nitrogen uptake by symbiotic marine cnidarians:
753 a critical review. P. Roy. Soc. Lond. B. Bio. 237, 109-125.
754 Moller, S.G., 2005. Plastids: Annual Plant Reviews. Volume thirteen. John Wiley, 344 pp.
755 Muscatine, L., D'Elia, C.E., 1978. The uptake, retention and release of ammonium by reef
756 corals. Limnol. Oceanogr. 23, 725–734.
757 Muscatine, L., Masuda, H., Burnap, R., 1979. Ammonium uptake by symbiotic and
758 aposymbiotic reef corals. B. Mar. Sci. 29, 572-575.
759 Newsholme, P., Lima, M.M.R., Procopio, J., Pithon-Curi, T.C., Bazotte, R.B., Curi, R., 2003.
760 Glutamine and glutamate as vital metabolites. Braz. J. Med. Biol. Res. 36, 153-63.
761 Norton, J.H., Shepherd, M.A., Long, H.M., Fitt, W.K., 1992. The zooxanthellal tubular system
762 in the giant clam. Biol. Bull. 183, 503–506.

763 Onate, J.A., Naguit, M.R.A., 1989. A preliminary study on the effect of increased nitrate
764 concentration on the growth of giant clams *Hippopus hippopus*. In: Zaragoza, E. C., de
765 Guzman, D. L., Gonzales, E. P. [Eds.]. Culture of Giant Clams (Bivalvia: Tridacnidae).
766 Australian Centre for International Agricultural Research, Canberra, pp. 57–61.
767 Poo, J.S., Choo, C.Y., Hiong, K.C., Boo, M.V., Wong, W.P., Chew, S.F., Ip, Y.K., 2020.
768 Phototrophic potential and form II ribulose-1, 5-bisphosphate carboxylase/oxygenase
769 expression in five organs of the fluted giant clam, *Tridacna squamosa*. Coral Reefs 39,
770 361-374.
771 Poo, J.S.T., Boo, M.V., Chew, S.F., Ip, Y.K., 2021. Using form II ribulose-1,5-bisphosphate
772 carboxylase/oxygenase to estimate the phototrophic potentials of *Symbiodinium,*
773 *Cladocopium and Durusdinium* in various organs of the fluted giant clam, *Tridacna*
774 *squamosa*, and to evaluate their responses to light upon isolation from the host. Coral
775 Reefs. doi: 10.1007/s00338-020-02031-4
776 Rees, T.A., Fitt, W.K., Yellowlees, D., 1994. Host glutamine synthetase activities in the giant
777 clam. Zooxanthellae symbiosis: effects of clam size, elevated ammonia and continuous
778 darkness. Mar. Biol. 118, 681-685.
779 Rossbach, S., Saderne, V., Anton Gamazo, A., Duarte, C.M., 2019. Light-dependent
780 calcification in Red Sea giant clam *Tridacna maxima*. Biogeosciences 16, 2635–2650.
781 Rossbach, S., Subedi, R.C., Ng, T.K., Ooi, B.S., Durarte, C.M. 2020. Iridocytes mediate
782 photonic cooperation between giant clams (Tridacninae) and their photosynthetic
783 symbionts. Front. Mar. Sci. 7:465. doi: 10.3389/fmars.2020.00465
784 Schiaffino, S., Dyar, K.A., Ciciliot, S., Blaauw, B., Sandri, M., 2013. Mechanisms regulating
785 skeletal muscle growth and atrophy. FEBS J. 280, 4294-4314.

786 Shepherd, D., Leggat, W., Rees, T.A.V., Yellowlees, D., 1999. Ammonium, but not nitrate,
787 stimulates an increase in glutamine concentration in the haemolymph of *Tridacna gigas*.
788 Mar. Biol. 133, 45–53.
789 Shoguchi, E., Beedessee, G., Tada, I., Hisata, K., Takeshi, K., Takeshi, T., Arakaki, N., Fujie,
790 M., Koyanagi, R., Roy, M.C., Kawachi, M., Hidaka, M., Satoh, N., Shinzato, C., 2018.
791 Two divergent *Symbiodinium* genomes reveal conservation of a gene cluster for
792 sunscreen biosynthesis and recently lost genes. BMC Genomics 19, 458.
793 Stasek, C.R., 1962. The form, growth and evolution of the Tridacnidae (Giant Clams). Arch.
794 Zool. Exp. Gen. 101, 01-40.
795 Summons, R.E., Boag, T.S., Osmond, C.B., 1986. The effect of ammonium on photosynthesis
796 and the pathway of ammonium assimilation in *Gymnodinium microadriaticum* in vitro
797 and in symbiosis with tridacnid clams and corals. P. Roy. Soc. Lond. B. Bio. 227, 147-
798 159.
799 Szmant, A.M., Gassman, N.J., 1990. The effects of prolonged "bleaching" on the tissue
800 biomass and reproduction of the reef coral *Montastrea annularis*. Coral Reefs 8, 217–
801 224.
802 Tabakaeva, O.V., Tabakaev, A.V., 2016. Amino-acid composition of soft tissues of the far-
803 east bivalve mollusk *Anadara broughtonii*. Chem. Nat. Compd. 52, 468-471.
804 Tang, Y.Z., Dobbs, F.C., 2007. Green autofluorescence in dinoflagellates, diatoms, and other
805 microalgae and its implications for vital staining and morphological studies. Appl.
806 Environ. Microb. 73, 2306-2313.
807 Taylor, L., Curthoys, N.P., 2004. Glutamine metabolism: role in acid-base balance. Biochem.
808 Mol. Biol. Educ. 32, 291–304.
809 Taylor, F.J.R., Hoppenrath, M., Saldarriaga, J.F., 2008. Dinoflagellate diversity and
810 distribution. Biodivers. Conserv. 17, 407-418.

811 Tischner, R., Hüttermann, A., 1980. Regulation of glutamine synthetase by light and during
812 nitrogen deficiency in synchronous *Chlorella sorokiniana*. Plant physiol. 66, 805-808.
813 Vander Heiden, M.G., DeBerardinis, R.J., 2017. Understanding the intersections between
814 metabolism and cancer biology. Cell 168, 657-669.
815 Wang, J.T., Douglas, A.E., 1999. Essential amino acid synthesis and nitrogen recycling in an
816 alga–invertebrate symbiosis. Mar. Biol. 135, 219-222.
817 Weber, M., 2009. The biogeography and evolution of *Symbiodinium* in giant clams
818 (Tridacnidae). Ph.D. dissertation, University of California, Berkeley, 67 pp.
819 Wilkerson, F.P., Muscatine, L., 1984. Uptake and assimilation of dissolved inorganic nitrogen
820 by a symbiotic sea anemone. P. Roy. Soc. Lond. B. Bio. 221, 71-86.
821 Wilkerson, F.P., Trench, R.K., 1986. Uptake of dissolved inorganic nitrogen by the symbiotic
822 clam *Tridacna gigas* and the coral *Acropora* sp. Mar. Biol. 93, 237-246.
823 Wong, M.L., Medrano, J.F., 2005. Real-time PCR for mRNA quantitation. BioTechniques 39,
824 75-78.
825 Xiang, T., Lehnert, E., Jinkerson, R. E., Clowez, S., Kim, R. G., DeNofrio, J. C., Pringle, J.R.,
826 Grossman, A.R., 2020. Symbiont population control by host-symbiont metabolic
827 interaction in Symbiodiniaceae-cnidarian associations. Nat. Comm. 11:108. doi:
828 10.1038/s41467-019-13963-z

Acknowledgements

This study was supported by the Singapore Ministry of Education through grants to Y. K. Ip (R-154-000-A37-114 and R-154-000-B69-114) and to S. F. Chew (NIE AcRF RI3/19CSF).

Conflict of interest

The authors declare that the research was conducted in the absence of any commercial or financial relationships that could be construed as a potential conflict of interest.

835 Table 1. Ratios of the transcript level of *zooxanthellal Glutamine Synthetase 1* (*Zoox-GS1*) to that of *zooxanthellal form II ribulose-1,5-*
836 *bisphosphate carboxylase/oxygenase (Zoox-rbcII)* or that of *zooxanthellal Urease (Zoox-URE)* in five organs of *Tridacna squamosa*
837 exposed to light for 3 h. Results represent means ± SD (n=10). Means not sharing the same letter are significantly different (p-value<0.01
838 after Bonferroni adjustment).

839

	Outer mantle	Inner mantle	Foot muscle	Hepatopancreas	Ctenidium
Zoox-GS1/Zoox-rbcII ($x10^{-2}$)	0.82 ± 0.30^{ab}	0.92 ± 0.21^{ab}	1.03 ± 0.21^{b}	0.68 ± 0.17^{a}	0.98 ± 0.62^{ab}
Zoox-GS1/Zoox-URE	1.52 ± 1.06^{a}	4.16 ± 1.52^{c}	3.86 ± 2.10^{bc}	2.11 ± 0.78^{ab}	2.77 ± 1.45^{abc}

840

Fig. 1. Immunolabeling of zooxanthellal Glutamine Synthetase 1 (Zoox-GS1), which comprised GS1 of *Symbiodinium*, *Cladocopium* and *Durusdinium*, in the outer mantle of *Tridacna squamosa*. (A) Differential interference contrast (DIC) image overlaid with DAPI nuclear stain ('n' refers to the nucleus of a zooxanthella, ZX; 'N' refers to the nucleus of a zooxanthellae tubule, ZT) and red channel ('PL' refers to the plastid of the zooxanthella). (B) Zoox-GS1 immunolabeling in green. (C) Composite image of Zoox-GS1 immunolabeling with DIC and DAPI, with (D) a magnified view. (E) Validation of Zoox-GS1 in the cytoplasm and regions near the plasma membrane of symbiotic dinoflagellates by a peptide competition assay (PCA). Arrowheads indicate Zoox-GS1 immunolabeling concentrated near regions of the plasma membrane of symbiotic dinoflagellates while arrows indicate Zoox-GS1 immunolabeling in the cytoplasm. Scale bar: 20 μm.

Fig. 2. Transcript levels ($\times 10^3$ copies per ng total RNA) of *zooxanthellal Glutamine Synthetase 1* (*Zoox-GS1*), which comprised *GS1* of *Symbiodinium*, *Cladocopium* and *Durusdinium*, from the outer mantle (OM), inner mantle (IM), foot muscle (FM), hepatopancreas (HP) and ctenidium (CT) of *Tridacna squamosa* exposed to light for 3 h. Results represent means + S.E.M. (n=10). Means not sharing the same letter are significantly different from each other (p-value<0.05).

Fig. 3. Transcript levels (copies per ng total RNA) of *zooxanthellal Glutamine Synthetase 1* (*Zoox-GS1*), which comprised *GS1* of *Symbiodinium*, *Cladocopium* and *Durusdinium*, from (A) the outer mantle, (B) the inner mantle, and (C) the foot muscle of *Tridacna squamosa* kept in darkness for 12 h (control), or exposed to light for 3, 6 or 12 h. Results represent means + S.E.M. (n=4). Means not sharing the same letter are significantly different from each other (p-value<0.05).

Fig. 4. Protein abundance of zooxanthellal Glutamine Synthetase 1 (Zoox-GS1), which comprised GS1 of *Symbiodinium, Cladocopium* and *Durusdinium,* from (A) the outer mantle, (B) the inner mantle, and (C) the foot muscle of *Tridacna squamosa* kept in darkness for 12 h (control) or exposed to light for 3, 6 or 12 h. (i) An immunoblot of Zoox-GS1 of the specific organ. (ii) Relative normalized Zoox-GS1 protein abundance (a.u.) from the outer mantle, inner mantle or foot muscle. Results represent means + S.E.M. (n=4). Means not sharing the same letter are significantly different from each other (p-value<0.05).

874 Fig. 1

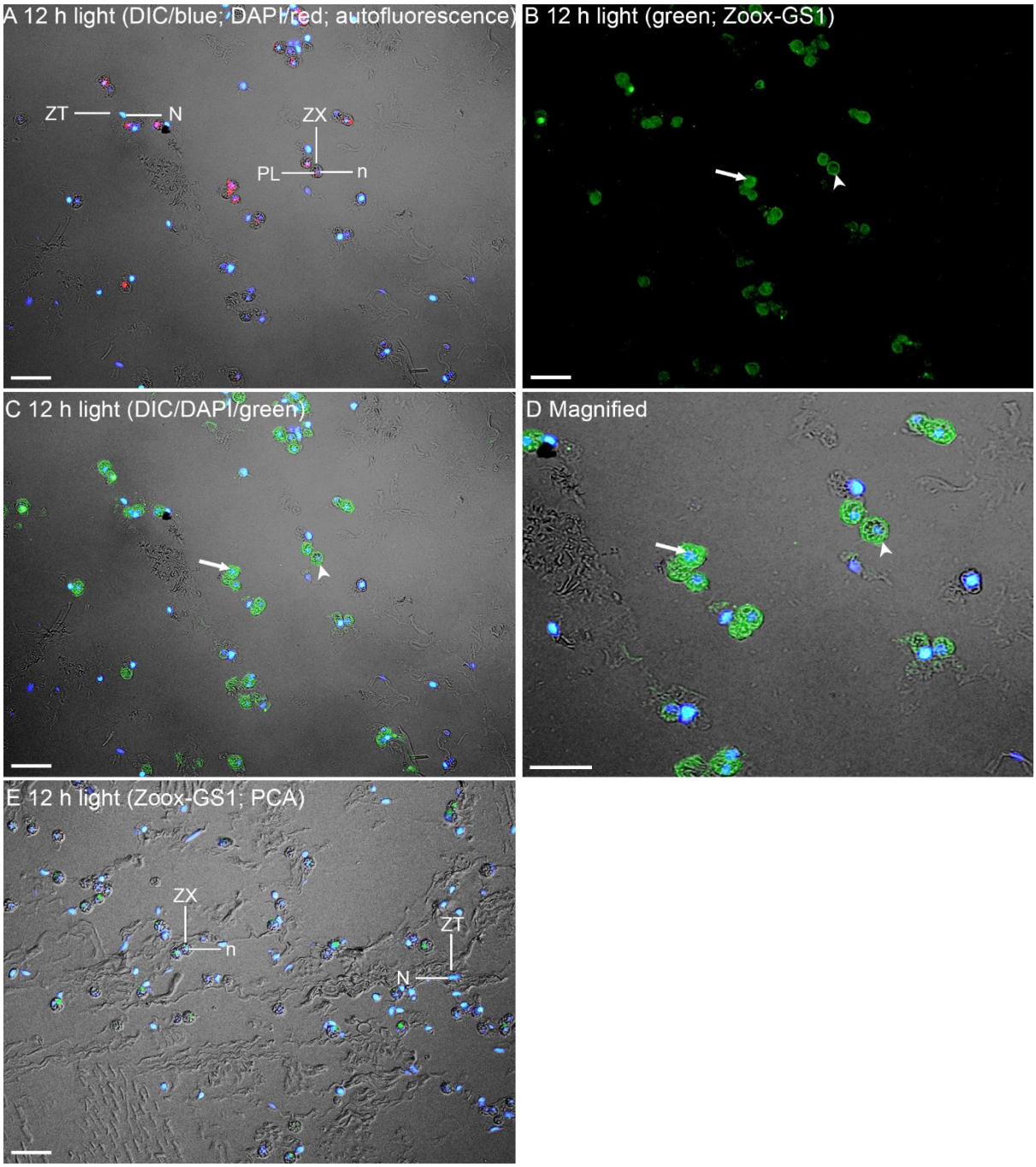

875

876

877 Fig. 2

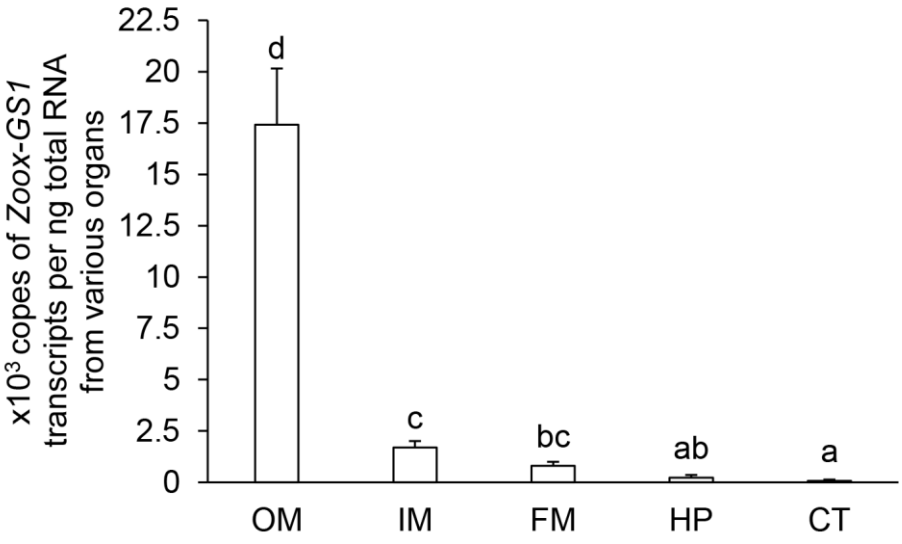
x10³ copes of Zoox-GS1 transcripts per ng total RNA from various organs
22.5
20
17.5
15
12.5
10
7.5
5
2.5
0
d
c
bc
ab
a
OM
IM
FM
HP
CT

878

879
880

Fig. 3

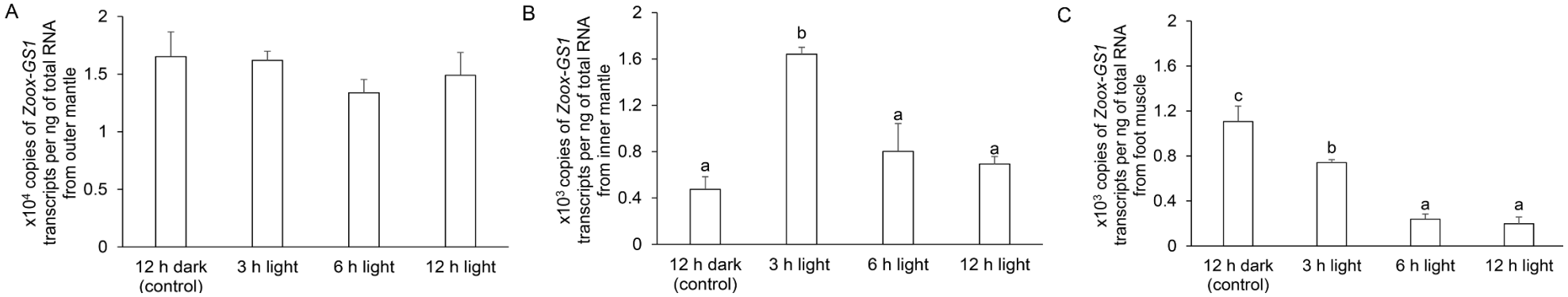

881

882

Fig. 4

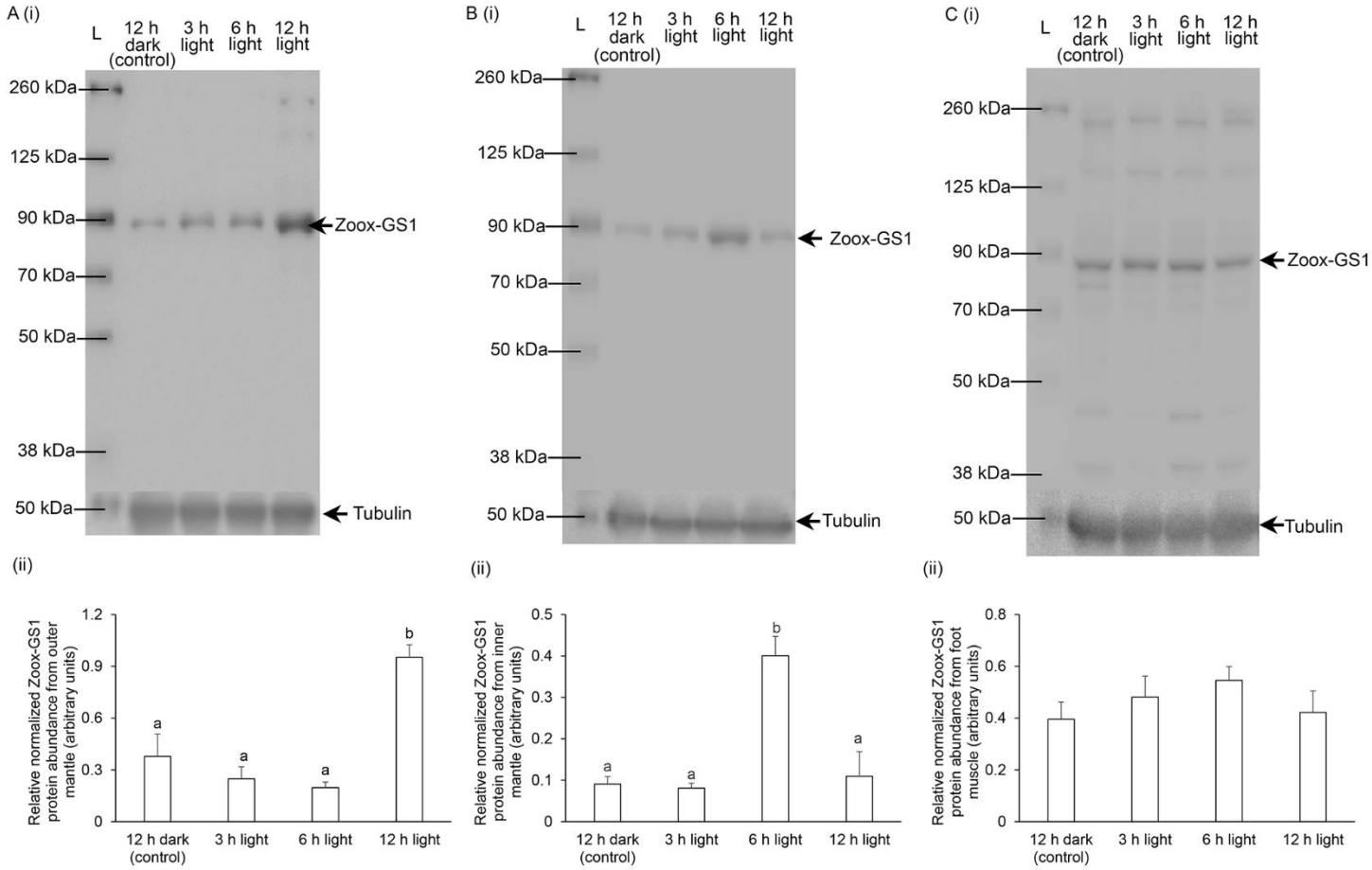
A (i)
L
12 h dark (control)
3 h light
6 h light
12 h light
260 kDa
125 kDa
90 kDa
70 kDa
50 kDa
38 kDa
50 kDa
Zoox-GS1
Tubulin
(ii)
Relative normalized Zoox-GS1 protein abundance from outer mantle (arbitrary units)
1.2
0.9
0.6
0.3
0
a
a
a
b
12 h dark (control)
3 h light
6 h light
12 h light
B (i)
L
12 h dark (control)
3 h light
6 h light
12 h light
260 kDa
125 kDa
90 kDa
70 kDa
50 kDa
38 kDa
50 kDa
Zoox-GS1
Tubulin
(ii)
Relative normalized Zoox-GS1 protein abundance from inner mantle (arbitrary units)
0.5
0.4
0.3
0.2
0.1
0
a
a
b
a
12 h dark (control)
3 h light
6 h light
12 h light
C (i)
L
12 h dark (control)
3 h light
6 h light
12 h light
260 kDa
125 kDa
90 kDa
70 kDa
50 kDa
38 kDa
50 kDa
Zoox-GS1
Tubulin
(ii)
Relative normalized Zoox-GS1 protein abundance from foot muscle (arbitrary units)
0.8
0.6
0.4
0.2
0
12 h dark (control)
3 h light
6 h light
12 h light

883

Supplementary Table S1. Amino acid similarity between Glutamine Synthetase 1 (GS1) sequences retrieved from various dinoflagellate databases and the epitope sequence used to generate the custom-made anti-TSZGS1 antibody. The epitope sequence DGVTRSKTMTMTAR was designed at a conserved region of five GS1 sequences (with their contig numbers listed). Two *Symbiodinium* GS1 sequences were obtained from Bayer et al. (2012) and Shoguchi et al. (2018), two *Cladocopium* GS1 sequences were obtained from Levin et al. (2016) and Shoguchi et al. (2018), and one *Durusdinium* GS1 sequence was obtained from Ladner et al. (2012).

Sequence contig number in the respective database	Number of amino acid matches between sequence and epitope, with percentage (%) match in parenthesis
Symbiodinium GS1 sequences	
Comp26637	12/14 (85.7)
kb8 rep c6248	12/14 (85.7)
Cladocopium GS1 sequences	
Comp261010	13/14 (92.9)
TR64176	13/14 (92.9)
Durusdinium GS1 sequence	
GAFP01005926.1	13/14 (92.9)

Supplementary Table S2. Similarity between the epitope used to generate the custom-made anti-α-tubulin antibody and the amino acid sequences of α-tubulin from three genera of dinoflagellates and six species of molluscs. The epitope sequence PKDVNAAVATIKTK was selected at a conserved region of all α-tubulin sequences examined. Sequences of α-tubulin of dinoflagellates were obtained from various online dinoflagellate databases, whereby, two *Symbiodinium* α-tubulin sequences were obtained from Aranda et al. (2016); two *Cladocopium* α-tubulin sequences were obtained from Shoguchi et al. (2018); and, two *Durusdinium* α-tubulin sequences were obtained from Ladner et al. (2012). Six α-tubulin sequences from molluscs (*Aplysia californica*, *Cepaea nemoralis*, *Crassostrea gigas*, *Crassostrea brasiliana*, *Patella vulgata*, and *Uroteuthis edulis*) were obtained from Genbank (with accession numbers listed).

Source of sequence (with contig number in the respective database for dinoflagellates)	Number of amino acid matches between sequence and the selected epitope for antibody production, with percentage (%) match in parenthesis
Symbiodinium	
kb8_rep_c48345	14/14 (100)
kb8_rep_c51196	14/14 (100)
Cladocopium	
comp27185_c0	14/14 (100)
comp22314_c2	14/14 (100)
Durusdinium	
d_sym_87768	14/14 (100)
d_sym_121557	14/14 (100)
Molluscs	

A. californica (NP_001191500.1)	13/14 (92.9)
C. nemoralis (AXI69343.1)	13/14 (92.9)
C. gigas (BAD80736.1)	13/14 (92.9)
C. brasiliana (AVF19943.1)	13/14 (92.9)
P. vulgate (CAA54712.1)	13/14 (92.9)
U. edulis (BAW15928.1)	13/14 (92.9)

Supplementary Table S3. Nucleotide similarity between *Glutamine Synthetase 1* (*GS1*) sequences obtained from various dinoflagellate databases and the *TSZGS1* comprehensive qPCR primer. The *TSZGS1* comprehensive qPCR primer (forward: 5'- GGAGCAAGGTCATGGAGGA -3'; reverse: 5'- ATCATCAAGTTCGGCGGC -3') was designed at a conserved region of all available *GS1* sequences from the databases (represented by their contig numbers). Three *Symbiodinium GS1* sequences were retrieved from Bayer et al. (2012), Aranda et al. (2016) and Shoguchi et al. (2018); two *Cladocopium GS1* sequences were obtained from Levin et al. (2016) and Shoguchi et al. (2018); and one *Durusdinium GS1* sequences was retrieved from Ladner et al. (2012).

Contig number in the respective database	Number of nucleotide matches between sequence and qPCR primer, with percentage (%) match in parenthesis	
	Forward primer	Reverse primer
Symbiodinium GS1 sequences		
Comp26637 c0 seq2	17 (89.5)	18 (100)
Smic2606	16 (84.2)	17 (94.4)
kb8 rep c6248	17 (89.5)	18 (100)
Cladocopium GS1 sequences		
TR64176 c0 g4 i1	19 (100)	16 (88.9)
comp261010 c1 seq1	19 (100)	16 (88.9)
Durusdinium GS1 sequence		
GAFP01005926.1	19 (100)	18 (100)

Supplementary Fig. S1. Peptide competition assay (PCA) on anti-Zoox-GS1 antibody. The presence of Zoox-GS1 band on an outer mantle sample exposed to 12 h of light (A) disappeared when anti-Zoox-GS1 antibody was neutralized with immunizing peptide (B).

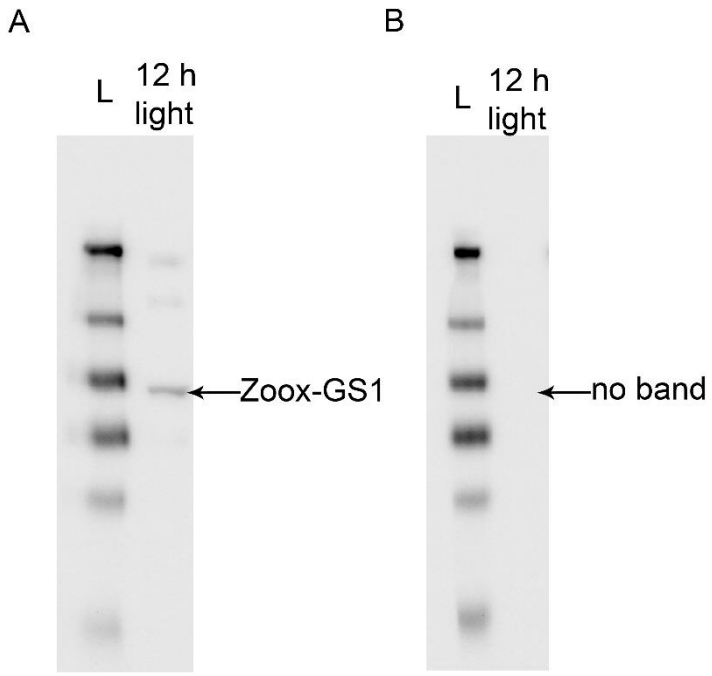

Supplementary Fig. 2. Immunoblot showing the absence of the 85 kDa Zoox-GS1 protein band in extracts from hepatopancreas and ctenidium at 100 µg of protein load.